Poster #29

Reconstructing Seasonal Antarctic Sea Ice Extent during the 20th Century

Ryan L. Fogt and Amanda M. Sleinkofer

Department of Geography and Scalia Laboratory for Atmospheric Analysis, Ohio University, Athens, OH, USA

Introduction

- Continuous measurements of Antarctic sea ice, including its extent, begin around 1979 with the start of the modern satellite era
- Although short in duration, these satellite records showed an overall increase in sea ice with strong regional trends (including significant ice loss in some regions) prior to 2016
- In spring 2016, widespread ice loss occurred, and sea ice extent remained below normal until 2020
- These impressive trends need a longer history to better understand them, which is one of the main goals of creating seasonally resolved reconstructions of Antarctic sea ice extent

Figure 1

Fig. 1. Time series of the summer (DJF) and autumn (MAM) sea ice extent in the Weddell Sea sector from 1979-2015 (top row) and 1979-2018 (bottom row). Prior to 2016, there were statistically significant increases in sea ice extent in this region in DJF and MAM that disappeared after the decline in 2016 (Turner et al. 2020). Limited observations however make it difficult to know the uniqueness of these trends in the early 20th century prior to 1979.

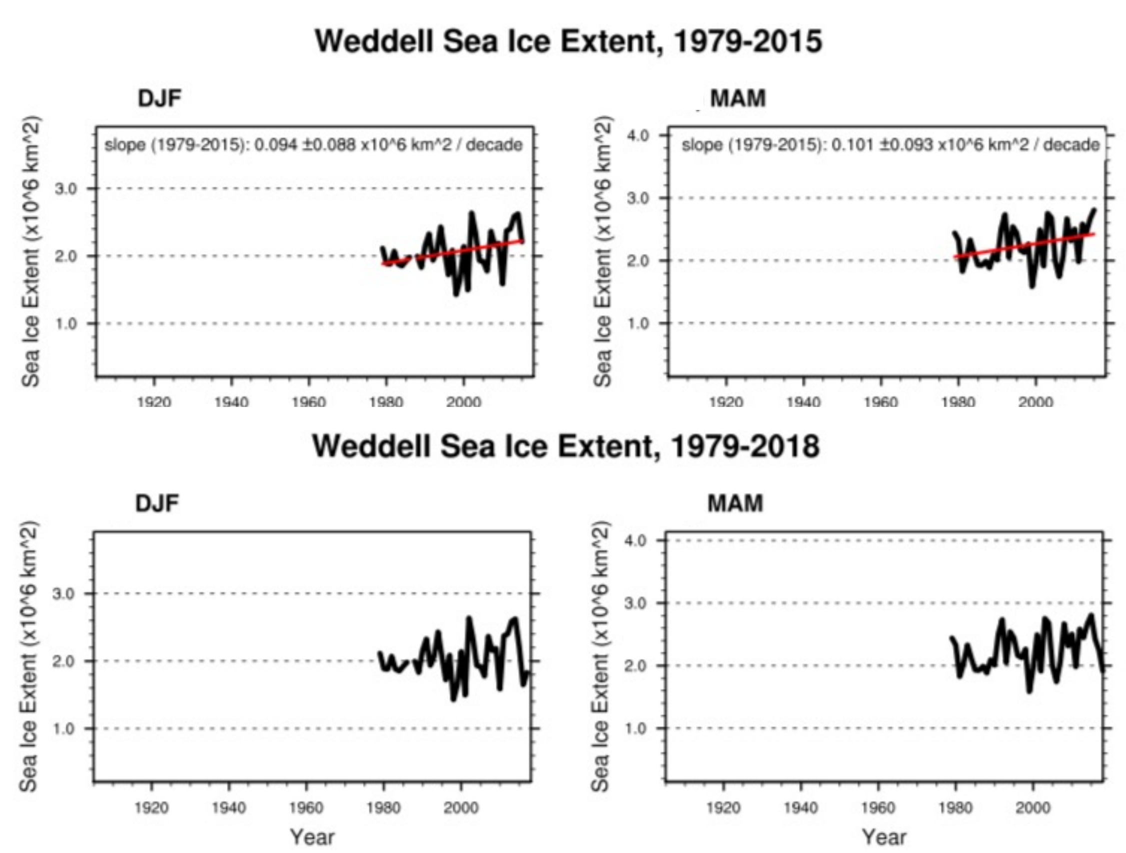

Data and Methods

- Long-term (beginning in at least 1905) seasonal mean temperature and pressure observations, as well as climate pattern indices known to influence Antarctic sea ice extent, were correlated with the seasonal sea ice extent time series for the sea ice sectors determined by Raphael and Hobbs (2014).
- **Lags** of up to 1 season (predictor data leading sea ice extent) were allowed to represent the physical processes in nature and indirectly account for the influence of the ocean on sea ice variability
- **Sensitivity to network sizes:** Only data that were correlated a certain significance thresholds ($p<0.10$, $p<0.05$, $p<0.025$, $p<0.01$) were retained for principal component analysis
- **Reconstruction generation:** A subset the most correlated principal components (PCs) with the sea ice series being reconstructed was then regressed onto the sea ice extent time series. Using the data through back to 1905 and the relationships these data share with the PCs used in the regression creates the reconstruction
- **Validation reconstruction:** The process was repeated but by predicting each year (withholding the 2 neighboring years before and after) to create an independent validation reconstruction; this procedure also determined where to cut the subset of PCs to avoid model over-fitting
- **Ensemble reconstruction:** data layers from the climate modes were subsequently added one at a time, if correlated, to create an ensemble of reconstructions, along with reconstructions from the various networks, giving up to 40 different reconstructions per sector and season

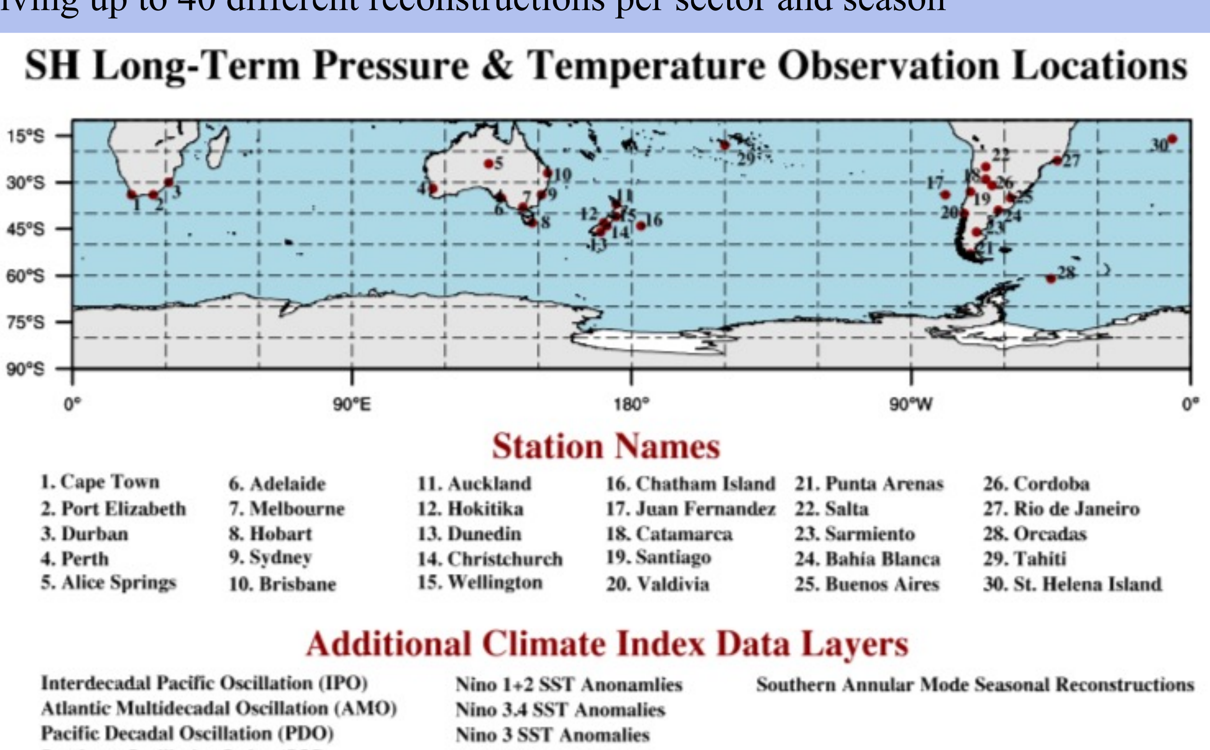

Figure 2

Fig. 2. Map of long-term pressure and temperature observations and listing of climate indices used in the seasonal Antarctic sea ice extent reconstructions.

Figure 3

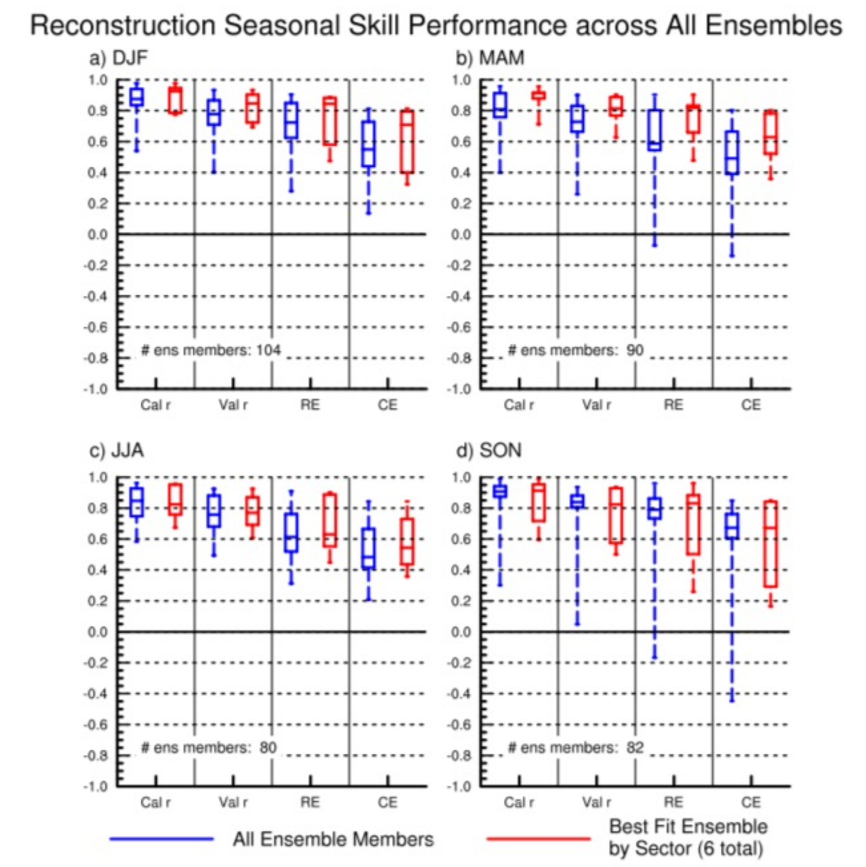

Fig. 3. Boxplots of reconstruction skill metrics across all ensemble members (blue) and the best fit reconstructions for each sector (red). Cal r = calibration correlation (correlation of reconstruction with sea ice extent); Val r = validation reconstruction (correlation of validation reconstruction with sea ice extent); RE = reduction of error; CE = coefficient of efficiency. RE and CE range from negative infinity to +1, with values above zero indicating performance above the climatological mean for the reconstruction and validation reconstruction, respectively.

- In DJF and JJA all ensemble reconstructions add value beyond the climatological mean, and only a few outliers of low performance exist in MAM and SON
- The best fit reconstructions (determined here as the highest CE) all outperform the climatological mean

Figure 4

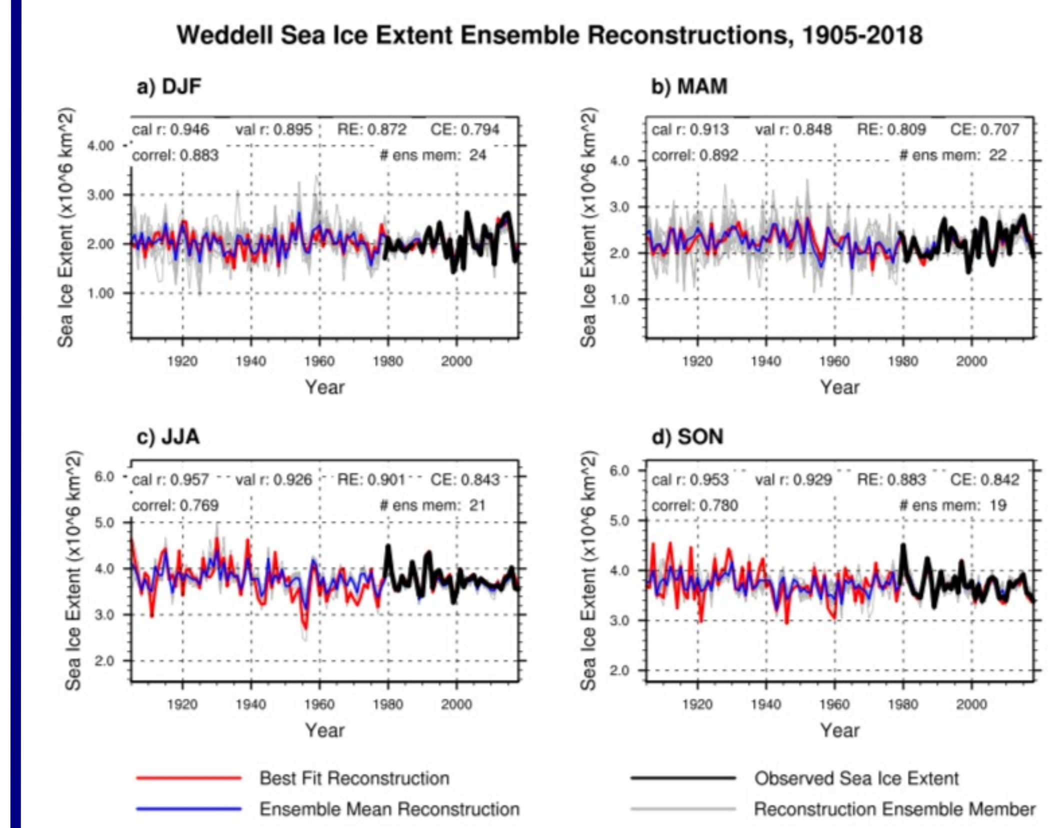

Fig. 4. Time series plots of seasonal Weddell Sea ice extent ensemble reconstructions (gray lines), best fit reconstruction (red) and the ensemble mean (blue), along with the observed sea ice extent (black). The skill metrics from Fig. 3 are given for the best fit reconstruction, as well as the correlation between the best fit and ensemble mean reconstructions (correl) and the number of ensemble members for each season

- The Weddell Sea is one of the higher performing reconstructions, with larger numbers of ensembles and stronger connections to pressure and temperature
- The temperature at nearby station Orcadas (Fig. 2) is an important predictor for sea ice in this sector, which improves its skill
- The impressive changes in the short observed record (Figure 1) can now be confidently placed in a longer historical context (Figure 3)

Figure 5

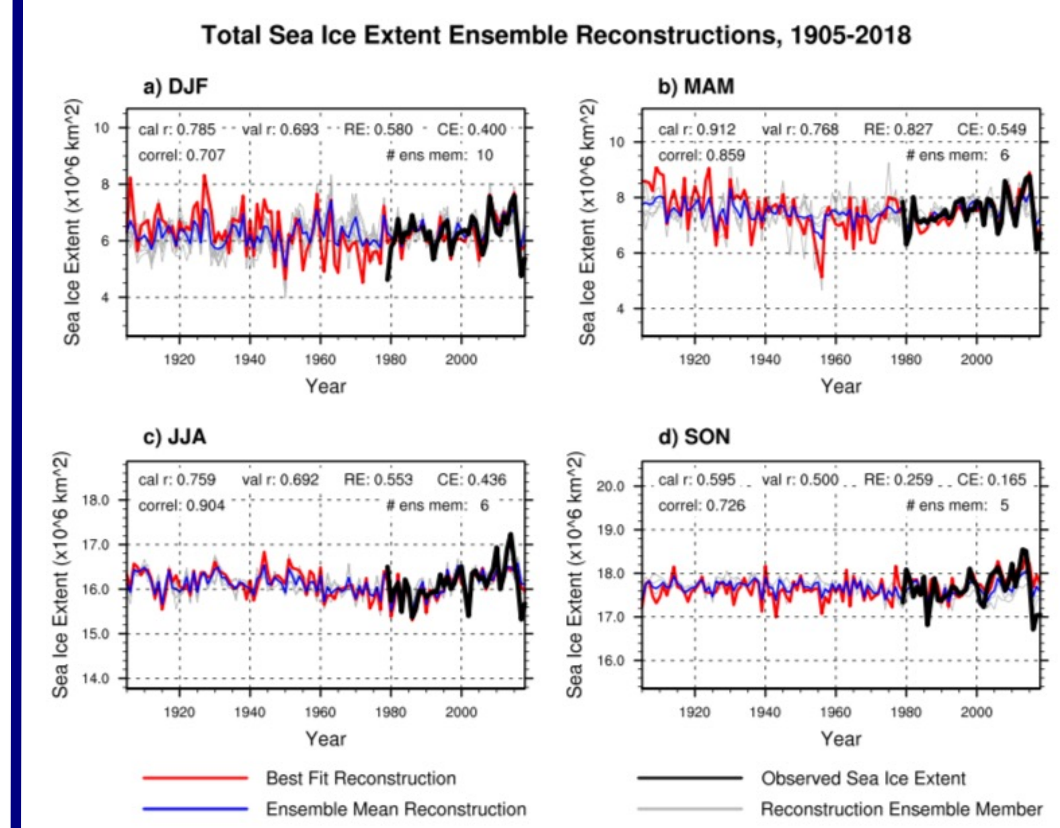

Fig. 5. As in Fig. 4, but for the seasonal total Antarctic sea ice extent.

- The Total sea ice extent is one of the lower performing reconstructions overall, and the lowest performing in SON. This could be due to:
  - Fewer ensemble members leading to less predictive power (less relationships with observations and large-scale climate overall)
  - The fact that sea ice responds more regionally to localized forcing in both the atmosphere and ocean, whereas total sea ice represents the sum of many distinct regional processes in Antarctic sea ice, which are not easily predicted
  - The decline in 2016 is especially pronounced in the total sea ice extent time series, yet it is unlikely that any predictor (and their related PCs) would have such a dramatic decline.
- Nonetheless, the Total sea ice extent reconstructions still add value beyond the climatological mean and can be used if care is given to their larger uncertainty

Figure 6

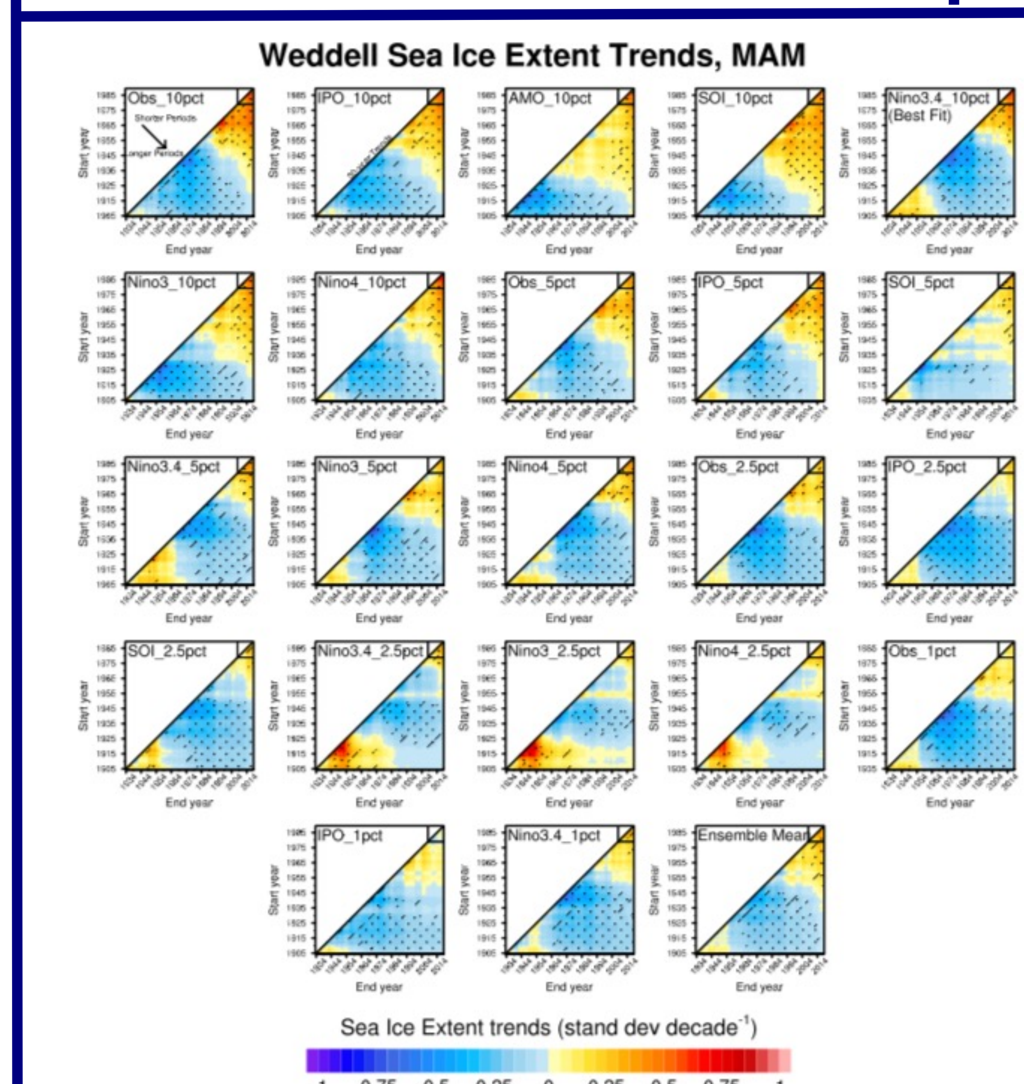

Fig. 6. Trends for 30+ years (shading) for the various ensemble reconstructions for the Weddell Sea ice extent in MAM. The y-axis indicates the starting year and the x-axis the ending year for the trend; shorter time periods are in the upper left of each panel and longer time periods are in the bottom right. The diagonal line represents 30 years exactly. The name for each ensemble is given in the panel, as well as the best fit and ensemble mean reconstructions. Cross-hatching indicates trends significantly different from zero at $p<0.10$, stippling indicates trends different from zero at $p<0.05$.

- Although there are differences between the ensemble members, there is general agreement that the sea ice gains in the observed period (boxes in the upper right of each panel) are strongly contrasted to sea ice losses (or at least sea ice extent retreat) in the Weddell Sea in the early 20th century
- Most ensemble members and the ensemble mean also show significant ($p<0.10$) sea ice extent decreases throughout 1905-2018 in MAM for the Weddell Sea.

Summary and Conclusions

- Sea ice extent reconstructions using a principal component regression technique are possible, providing value in all seasons and sectors beyond the climatological mean
- The reconstruction skill varies by sector and season, with larger data predictor data networks ($p<0.10$) and ensemble member sizes commonly performing better than smaller but more highly correlated data networks
- These ensemble reconstructions open new doors for further research in understanding the historical behavior of Antarctic sea ice which will help place the current changes in a longer context and hopefully improve our near and long-term prediction of future Antarctic sea ice extent
- Work for a monthly sea ice extent reconstruction back until 1957 incorporating Antarctic observations, and a seasonal sea ice concentration reconstruction back until 1950 is ongoing

References

- Raphael, M. N., and W. Hobbs, 2014: The influence of the large-scale atmospheric circulation on Antarctic sea ice during ice advance and retreat seasons. *Geophys. Res. Lett.*, **41**, 5037–5045, https://doi.org/10.1002/2014GL060365.
- Turner, J., and Coauthors, 2020: Recent Decrease of Summer Sea Ice in the Weddell Sea, Antarctica. *Geophys. Res. Lett.*, **47**, https://doi.org/10.1029/2020GL087127.

Acknowledgements

- All authors acknowledge support from the National Science Foundation Office, grant number PLR-1744998.

fogtr@ohio.edu